NJC

Accepted Manuscript

This article can be cited before page numbers have been issued, to do this please use: J. Jiao, A. Wang, M. Chen, M. Wang and C. Yang, *New J. Chem.*, 2019, DOI: 10.1039/C9NJ00574A.

ROYAL SOCIETY OF CHEMISTRY

rsc.li/njc

New Journal of Chemistry

View Article Online
DOI: 10.1039/C9NJ00574A

PAPER

Novel 5-chloro-pyrazole derivatives containing a phenylhydrazone moiety as potent antifungal agents: Synthesis, crystal structure, biological evaluation and 3D-QSAR study

Received 00th January 20xx,
Accepted 00th January 20xx

DOI: 10.1039/x0xx00000x

www.rsc.org/

Jian Jiao,[a,b] An Wang,[b] Min Chen,[a,b] Meng-Qi Wang[b] and Chun-Long Yang [*,a,b]

Based on the active substructure combination principle, twenty-four novel 5-chloro-pyrazole derivatives containing a phenylhydrazone moiety were designed, synthesized, and evaluated for antifungal activity. Their structures were confirmed by ^{1}H NMR, ^{13}C NMR, and HR-MS spectra. And the single-crystal structure of compound **8a** was analyzed emphatically by X-ray diffraction. The antifungal activities against *Fusarium graminearum*, *Botrytis cinerea*, and *Rhizoctonia solani* were evaluated *in vitro.* The results of bioassay test revealed that most target compounds showed obvious fungicidal activity. Strikingly, the compound **7c** exhibited most potent activity with the EC_{50} values of 0.74, 0.68, and 0.85 μg mL^{-1} against above three plant pathogenic fungi, respectively. And the compounds **7c**, **8d,** and **8g** showed significant bioactivity against *R. solani* with the EC_{50} values of 0.85, 0.25, and 0.96 μg mL^{-1}, respectively. In addition, the CoMFA and CoMSIA molecular modelings were established for 3D-QSAR study and presented good predictive ability with q^2 values of 0.575 and 0.667, and r^2 values of 0.961 and 0.962, respectively. The results provided useful information for guiding the design and synthesis of novel potent pyrazole derivatives with good antifungal activity.

Introduction

Plant diseases cause severe crop yield reduction, deteriorate the agricultural products quality and result in economic losses in agriculture.[1,2] Some diseased crops even endanger human health.[3,4] With the development of modern agrichemical industry, the synthetic pesticides become the most important and effective measure to fight against plant diseases.[5–8] Such as carbendazim, dimethachlon and fludioxonil,[9] they are all frequently-used fungicides to control these diseases. However, the emergence of multiple drug-resistance and pesticide residues exposes the shortcoming of traditional pesticides.[10] This also indicates that the research and development of novel fungicides with highly efficient, good selectivity and eco-friendly properties is an urgent challenge in agriculture.

Pyrazole derivatives were widely used as pesticides in agrochemical chemistry and studied for years due to their broad-spectrum biological activities,[11] including antifungal,[12,13] insecticidal,[14] acaricidal,[15] antibacterial,[16] and herbicidal activities.[17] Meanwhile, the favorable chemical characteristics, convenient synthesis process and multiple reaction sites of pyrazole structure are also advantageous conditions for the design and synthesis of new pyrazole pesticides.[18,19] Some pyrazole-based fungicides, such as furametpyr, penthiopyrad, and pyrametostrobin, have contributed to the plant chemical protection (Fig. 1).[20,21] From these successful fungicide molecular models, it is speculated that the groups at the pyrazole ring, such as chlorine, methyl, and trifluoromethyl, especially the chlorine atom, may have positive effects on their biological activity. Some chloro-pyrazole derivatives containing the thiazole,[22] oxime ester,[23] hydrazine[24] or thiourea group[25] were found exhibiting obvious fungicidal activity.

Hydrazone is another substructure that has aroused our great concern. Some commercialized fungicides, such as ferimzone, drazoxolon, and benquinox (Fig. 1), contain the hydrazone moiety in their structures.[26,27] At the same time, it was found that introducing the hydrazone group into acetophenone,[28] nalidixic acid,[29] tetrahydro-*β*-carboline,[30] 1,2,3-triazole,[31] benzimidazole,[32] and quinoxaline[33] could effectively improve the antifungal activity of the target compounds. So far, only very few hydrazone fungicides have been used to control plant diseases, which makes it significant to research new fungicidal molecules with a hydrazone moiety.

In view of the above-mentioned research findings, the 5-chloro-1*H*-pyrazole formaldehydes with another common group chlorine, methyl or trifluoromethyl at 3-position were prepared firstly in this work. Then, the substituted phenylhydrazone moieties were respectively introduced at 4-

[a] Jiangsu Key Laboratory of Pesticide Science, Nanjing Agricultural University, Nanjing, 210095, PR China.
[b] Department of Chemistry, College of Sciences, Nanjing Agricultural University, Nanjing, 210095, PR China.
[c] * Corresponding author. E-mail address: ycl@njau.edu.cn (C.L. Yang)

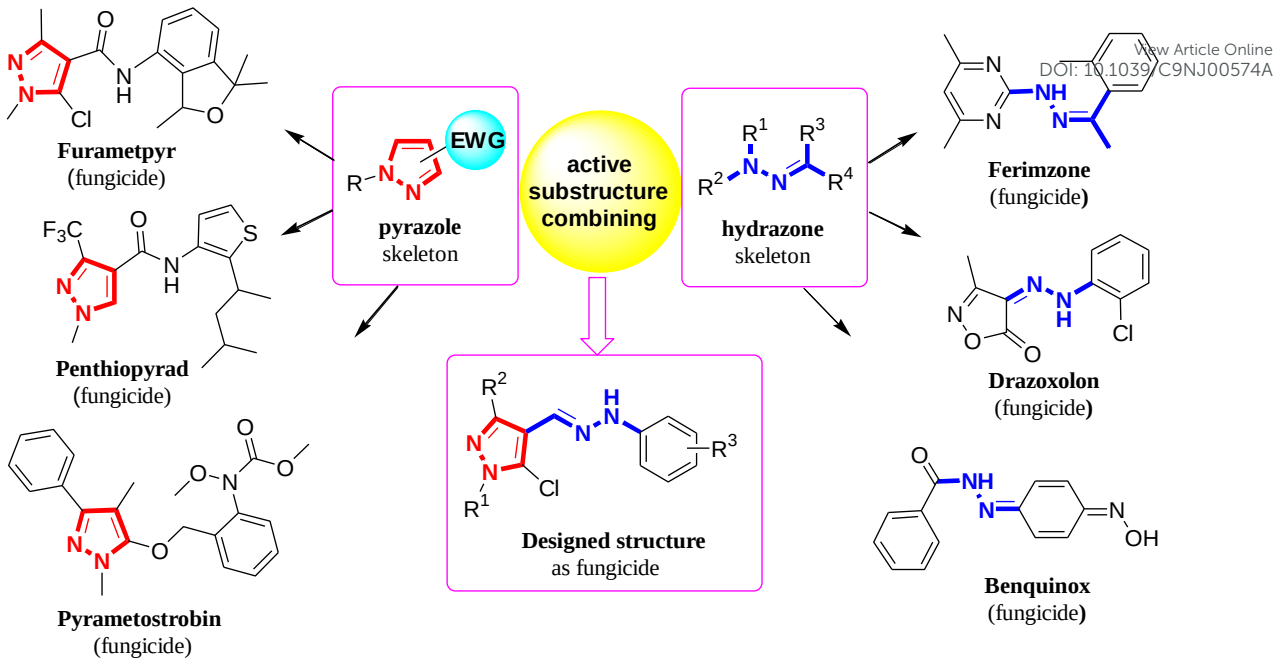

Fig. 1 Design strategy of target structures.

position of above pyrazole intermediates to design and synthesize a series of novel 5-chloro-1*H*-pyrazole derivatives containing a phenylhydrazone moiety for screening the antifungal activity against plant pathogenic fungi (Scheme 1). In addition, the CoMFA and CoMSIA models were established in Tripos's Sybyl X-2.1 software to analyse the 3D-QSAR (three dimensional quantitative structure-activity relationship) of target compounds based on antifungal activity against *R. solani*.[34–36]

Results and discussion

Synthesis of title compounds

The intermediates 3,5-dichloro-1*H*-pyrazole-4-carbaldehydes **3** were successfully achieved through cyclization by lactonization, acidification and Vilsmeier-Haack-Arnold reaction starting from diethyl malonate (Scheme 1).[37,38] The Vilsmeier-Haack-Arnold reaction was the key step of reaction route. According to the known procedure, the mole ratio of pyrazolidine-3,5-dione, DMF and $POCl_3$ was 1: 2: 3, and the reaction proceeded at 85 ℃ for 5 h.[37] The intermediates **3** were tried to be prepared with the same method, but the experiments showed that all the yields in these conditions were very low. Hence, the synthesis method of intermediates **3** was further optimization. Considering both 3 and 5-positions of intermediates **3** would be replaced by chlorine atoms, the amount of $POCl_3$ was tried to be enlarged gradually. Since the low solubility of intermediates **2** in DMF, the amount of solvent DMF was tried to be increased. Meanwhile, we found raising the reaction temperature can also increase the yield. As summarized in Table 1, the results indicated that the reaction proceeded readily in an appropriate solution system of ketone/DMF/$POCl_3$ (their mole ratio = 1: 4: 4) at 50 ℃ for 5 h, then 120 ℃ for 10 h, to give the expected intermediate **3a** in 40.6% yield.

The intermediates 5-chloro-1-methyl-1*H*-pyrazole-4-carbaldehydes **6** were prepared using the similar reaction steps as intermediates **3**, but using ethyl 4,4,4-trifluoroacetoacetate and ethyl acetoacetate as the starting materials, respectively (Scheme 1).[37,38] The Vilsmeier-Haack-Arnold reaction conditions were optimized too. In order to make the heating process less intense, segmental heating was adopted. As summarized in Table 1, the reaction was carried out in the solution system of ketone/DMF/$POCl_3$ (their mole ratio = 1: 2: 3) at 50 ℃ for 5 h, then 90 ℃ for another 5 h, to present the expected intermediates **6a** and **6b** in high yields of 80.25% and 77.60%, respectively (Table 1).

The twenty-four target compounds **7a–7q** and **8a–8g** were synthesized by the reaction of compound **3** or **6** with nine substituted phenylhydrazines respectively in ethanol under reflux for 2 h. The reaction progress was monitored by TLC (ethyl acetate/petroleum = 1: 4, v/v). Finally, the desired target compounds were obtained by recrystallization from the mixed solution of ethyl acetate/petroleum (v/v, 1: 8) with the yields ranging from 50.31% to 72.53%. This reaction was quite

Table 1 Optimization of preparation methods of intermediates **3** and **6**

Entry	Compd.	Ratio[a]	Temp (℃)	Yield (%)
1	**3a**	1: 2: 3	90	trace
2	**3a**	1: 2: 4	90	trace
3	**3a**	1: 4: 4	90	15.55
4	**3a**	1: 4: 6	90	15.06
5	**3a**	1: 4: 4	120	40.06
6	**6a**	1: 2: 3	90	80.25
7	**6b**	1: 2: 3	90	77.60

[a] Mole ratio of corresponding ketone: DMF: $POCl_3$.

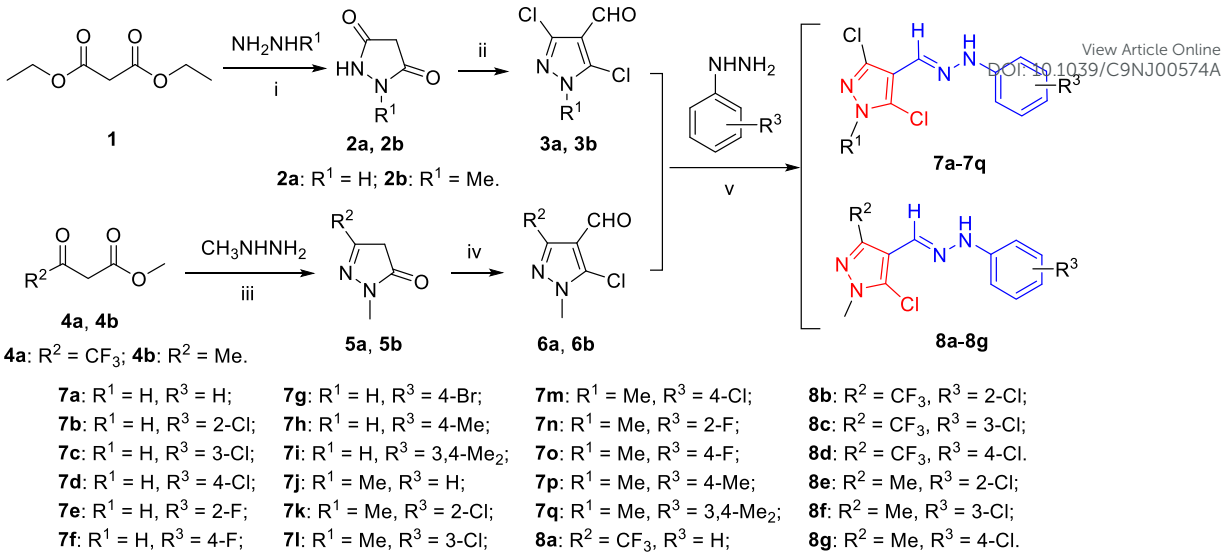

Scheme 1 Synthetic route to target compounds. *Reagents and conditions*: (i) C_2H_5OH, rt, 5 h; CH_3ONa, reflux, 8 h; 36% aq. HCl. (ii) DMF, $POCl_3$, 50 ℃, 5 h; 120 ℃, 10 h. (iii) C_2H_5OH, reflux, 8 h. (iv) DMF, $POCl_3$, 50 ℃, 5 h; 90 ℃, 5 h. (v) C_2H_5OH, reflux, 2 h.

convenient and efficient. The structures of all target compounds were confirmed by the spectroscopic data of ^1H NMR, ^{13}C NMR and HR-MS.

Single crystal structure of compound 8a

The crystallographic data of compound **8a** was listed in Table S1 of the supplementary information. As shown in Fig. 2, the compound **8a** crystallized with two independent molecules (Molecules A and B) in the asymmetric unit. The structure parameters of molecules A and B were consistent in bond distances (Table S1) and bond angles (Table S2). A intramolecular hydrogen bond was formed in molecule B [C(17)–H(17B)···Cl(2), Table 2], whereas this inter-atomic force was not found in molecule A which should attribute to the rotation of N(1)–C(5) single bond. Interestingly, the angles between the benzene and pyrazole were 5.705(93)° and 7.668(99)° in molecules A and B, respectively. Besides, the molecular ellipsoid of Molecule A and Molecule B both illustrated that the C=N–NH bond bears a (*E*)-configuration.

As shown in Fig. 3A, the crystal packing diagram of compound **8a** showed two intermolecular forces including the intermolecular hydrogen bonds and the π···π stacking interactions. The neighboring molecules A and B were connected by the intermolecular hydrogen bonds N(8)–H(8A)···N(2) and C(10)–H(10)···F(6) (Table 2). Besides, the molecules A were stacked up by the face-to-face π···π interactions which interacted on the benzene and pyrazole. The centroid-centroid distance of the benzene and pyrazole was 3.7182(2) Å, and the dihedral angle was 5.705(87)°. The same intermolecular force was applied to B, of which the centroid-centroid distance and the dihedral angle were 3.7475(2) Å and 7.668(100)°, respectively. It could be concluded that the molecules packing by the π···π stacking interactions were parallel absolutely. These different interactions connected the molecules and constituted a stable 3D network structure with cavities (Fig. 3B).

Table 2 Hydrogen bond distances (Å) and angles (°) of compound **8a**

D–H···A	*d*(D–H)	*d*(H···A)	*d*(D···A)	∠(DHA)
C(17)–H(17B)···Cl(2)	0.9600	2.8100	3.191(3)	104.6(2)
N(8)–H(8A)···N(2)[a]	0.8600	2.4900	3.212(4)	142.0(2)
C(10)–H(10)···F(6)[b]	0.9300	2.5000	3.119(4)	124.2(2)

[a] Symmetry code: -1+x, y, z; [b] Symmetry code: x, -1+y, 1+z.

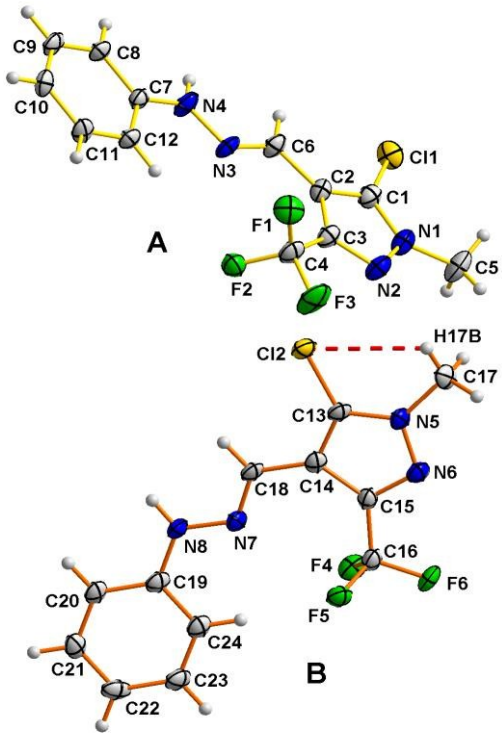

Fig. 2 ORTEP diagram of compound **8a**.

View Article Online
DOI: 10.1039/C9NJ00574A

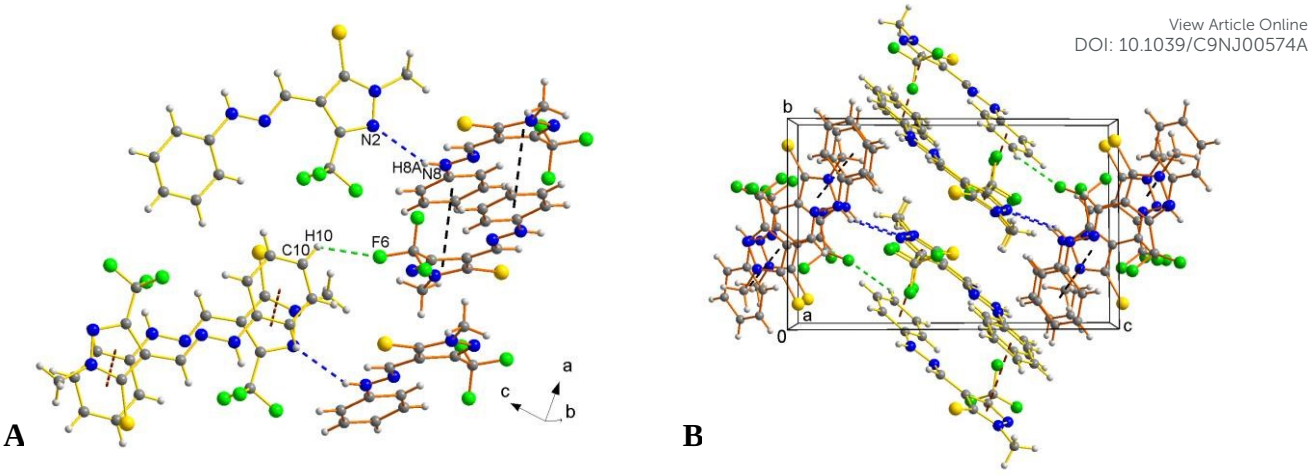

Fig. 3 Crystal packing diagram of compound **8a** showing intermolecular forces.

In vitro antifungal activity

The antifungal activities of target compounds **7a**–**7q** and **8a**–**8g** and the positive control fungicides carbendazim and penthiopyrad against *F. graminearum*, *B. cinerea* and *R. solani in vitro* were listed in Table 3.[39] The results in Table 3 suggested that most of the tested compounds exhibited obvious antifungal activities. The target compounds showed better bioactivity with the EC_{50} values of 0.25 μg mL^{-1} to 12.67 μg/mL against *R. solani* than these against other two fungi. Among them, the compounds **8d** exhibited potent activity against *R. solan*i with the EC_{50} value of 0.25 μg mL^{-1}, which is superior to that of carbendazim (0.54 μg mL^{-1}). The compounds **7c** and **8g** also showed good activity against *R. solan*i with the EC_{50} value of 0.85, and 0.96 μg mL^{-1}, respectively. In addition, the compounds **7c**, **7f**, and **8g** exhibited remarkable anti-*F. graminearum* activity with the EC_{50} values of 0.74, 0.85, and 0.94 μg mL^{-1}, respectively. The compounds **7c**, **7d**, **7g**, **7m**, and **7o** presented significant antifungal activity against *B. cinerea* with the EC_{50} values of 0.68, 0.87, 0.94, 0.85, and 0.84 μg mL^{-1}, respectively, which are close to 0.82 μg mL^{-1} of penthiopyrad. It is worth mentioning that the compound **7c** displayed potent activity with the EC_{50} values of 0.74, 0.68, and 0.85 μg mL^{-1} against above three tested fungi, respectively.

Table 3 Antifungal activity of target compounds against three phytopathogens

Compd.	EC_{50} (μg mL^{-1})[a]		
	F. graminearum	*B. cinerea*	*R. solani*
7a	4.60 ± 0.09	3.72 ± 0.09	2.31 ± 0.25
7b	10.75 ± 0.11	2.48 ± 0.07	3.17 ± 0.19
7c	0.74 ± 0.14	0.68 ± 0.26	0.85 ± 0.10
7d	1.64 ± 0.10	0.87 ± 0.11	1.38 ± 0.15
7e	5.56 ± 0.04	1.46 ± 0.35	1.74 ± 0.26
7f	0.85 ± 0.10	1.04 ± 0.21	1.37 ± 0.10
7g	2.11 ± 0.13	0.94 ± 0.07	1.28 ± 0.10
7h	10.21 ± 0.06	3.42 ± 0.05	4.73 ± 0.12
7i	14.66 ± 0.08	6.21 ± 0.04	12.67 ± 0.14
7j	9.91 ± 0.11	3.39 ± 0.03	1.97 ± 0.19
7k	19.30 ± 0.05	4.53 ± 0.03	5.99 ± 0.14
7l	6.95 ± 0.10	2.25 ± 0.06	2.23 ± 0.26
7m	1.16 ± 0.07	0.85 ± 0.21	1.07 ± 0.22
7n	18.42 ± 0.08	1.82 ± 0.20	2.65 ± 0.25
7o	1.09 ± 0.22	0.84 ± 0.06	1.16 ± 0.12
7p	4.49 ± 0.09	3.10 ± 0.04	2.86 ± 0.20
7q	7.67 ± 0.07	3.98 ± 0.05	6.67 ± 0.06
8a	15.39±0.17	14.39 ± 0.16	2.49 ± 0.05
8b	N.A.[b]	N.A.[b]	4.13 ± 0.15
8c	7.77 ± 0.08	7.47 ± 0.08	3.62 ± 0.17
8d	2.55 ± 0.35	3.99 ± 0.11	0.25 ± 0.26
8e	N.A.	N.A.	2.31 ± 0.11
8f	3.70 ± 0.45	5.61 ± 0.14	1.61 ± 0.05
8g	0.94 ± 0.12	3.49 ± 0.15	0.96 ± 0.05
Carbendazim	0.43 ± 0.18	0.42 ± 0.06	0.54 ± 0.11
Penthiopyrad	–	0.82 ± 0.17	–

[a] EC_{50} values were statistically analyzed using Excel and expressed as mean ± SD of triplicate experiment; [b] N.A. means no activity.

Qualitative SAR analysis

Some preliminary SAR (structure-activity relationship) rules were found and summarized as below. First, introducing a halogen atom into the 4-position of phenyl ring, such as 4-Cl, 4-F, or 4-Br group, can effectively enhance the antifungal activity of target compounds. In contrast, the presence of halogen atom at the 2-position of phenyl ring is unfavourable to increase the antifungal activity. Such as, the compounds **7d**, **7f**, **7g**, **7m**, **7o**, **8d**, and **8g** with a halogen atom at the 4-position of phenyl ring showed better activity than the compounds **7b**, **7e**, **7k**, **8b**, and **8e** with a halogen atom at the 2-position of phenyl ring. Second, introducing a methyl into the 3-position of pyrazole ring can enhance the antifungal activity. Such as the compounds **8e** and **8f** showed better activity than the compounds **8b** and **8c**. Therefore, the substituents at phenyl and pyrazole play a crucial role on the activity of 5-chloro-pyrazole derivatives containing a phenylhydrazone moiety.

3D-QSAR study

In order to understand in depth the relationship between structure and bioactivity of the target compounds, the fungicidal activity against *R. solani* was selected for the 3D-QSAR study by building the CoMFA and CoMSIA models. A total of twenty-four target compounds were randomly divided into training sets and test sets, including twenty-one and three

View Article Online
DOI: 10.1039/C9NJ00574A

compounds, respectively. The experimental and predicted pEC_{50} values for the training set and test set are reported in Table 4. The compound **8d** with best inhibitory activity against *R. solani* was selected as the template molecule, and its red bold structure in Fig. 4A was chosen as the common substructure to perform the alignment of training set molecules. The alignment result of all training set molecules is shown in Fig. 4B.

Based on the alignment, a series of molecular properties were calculated for the analysis. The statistical parameters

Table 4 Experimental and predicted pEC_{50} values of target compounds

Compd.	ApEC_{50}[b]	CoMFA		CoMSIA	
		PpEC_{50}[c]	R[d]	PpEC_{50}[c]	R[d]
7a	5.041	5.028	0.013	4.999	0.042
7b[a]	4.958	5.056	–0.098	5.549	–0.591
7c	5.528	5.452	0.076	5.300	0.228
7d	5.319	5.334	–0.015	5.319	0.000
7e	5.195	5.123	0.072	5.209	–0.014
7f	5.299	5.296	0.003	5.322	–0.023
7g	5.416	5.334	0.082	5.373	0.043
7h	4.754	4.848	–0.094	4.767	–0.013
7i	4.348	4.328	0.020	4.388	–0.040
7j	5.133	5.198	–0.065	5.149	–0.016
7k	4.703	4.821	–0.119	4.797	–0.094
7l	5.132	5.071	0.060	5.044	0.087
7m	5.451	5.488	–0.037	5.466	–0.015
7n	5.034	4.979	0.055	4.995	0.039
7o[a]	5.394	5.365	–0.029	5.340	–0.054
7p	4.994	4.979	0.015	4.916	0.078
7q	4.647	4.638	0.009	4.668	–0.021
8a	5.083	5.077	0.006	5.136	–0.053
8b	4.910	4.885	0.025	4.808	0.102
8c	4.968	4.946	0.022	5.026	–0.058
8d	6.130	5.953	0.177	5.889	0.241
8e	5.088	5.074	0.014	5.066	0.022
8f	5.244	5.311	–0.067	5.309	–0.066
8g[a]	5.422	5.169	0.253	5.748	–0.326

[a] Compounds in the test set. [b] Actual –log (EC_{50}). [c] Predicted –log (EC_{50}). [d] Residual.

were given in Table 5. The CoMFA model ($q^2 = 0.575$, $r^2 = 0.961$) was based on the steric and electrostatic fields, and the CoMSIA model ($q^2 = 0.667$, $r^2 = 0.962$) was based on the steric, electrostatic, hydrophobic, hydrogen bond donor and hydrogen bond acceptor fields. The PLS analysis was performed to establish a linear relationship between the molecular fields and the activity of molecules. The contour maps for the CoMFA and CoMSIA models are displayed in Fig. 5. And the correlation plots of CoMFA and CoMSIA models are shown in Fig. 6 and Fig. 7, respectively.

In the steric CoMFA map (Fig. 5A), green contours around 4-position (R^3) of phenyl ring, and 1 and 3-positions (R^1 and R^2) of pyrazole ring indicated that adding bulky substituents in these positions might enhance the antifungal activity. The yellow contour around 3-position of phenyl ring indicated that adding bulky substituents in this position might decrease the antifungal activity. This explained that the compounds **7m**, **7o**, **8d**, and **8g** had good anti-*R. solani* activity with the EC_{50} values of 1.07, 1.16, 0.25 and 0.96 μg/mL, respectively.

In the electrostatic CoMFA map (Fig. 5B), the red contours around 3 and 4-positions of phenyl ring indicated that the compounds with negative charge at these positions might have potent anti-*R. solani* activity. For example, the compounds **7c**, **7d**, **7f**, **7g**, **7m**, **7o**, **8d**, **8f**, and **8g** (with 3-halogen or 4-halogen at phenyl ring) exhibited higher antifungal activity than the compounds **7a**, **7h**, **7i**, **7j**, **7p**, and **7q** (with methyl or no substitution at 3 and 4-positions of phenyl ring). The blue contours around 3-positon of pyrazole ring, 2-position of phenyl ring and hydrazone group showed that the compounds with positive charge groups in these positions might have significant antifungal activity. Inversely, negative charge groups in these positions might weaken the activity, such as the compounds **7b**, **7k**, **8b**, and **8e** (R^3 = 2-Cl). Combined with the steric CoMFA map, it can indicate that the bulky groups with negative charges were favored at 4-position of phenyl ring and the groups with positive charges were favored at 3-position of pyrazole.

In the CoMSIA steric and electrostatic field equipotential maps (Fig. 5C and Fig. 5D), the effects of electronegativity groups and bulky groups at different positions on antifungal activity were also illustrated. In agreement with the electrostatic CoMFA map, the blue contour at 2-position of phenyl ring in Fig. 5D indicated that adding positive charge groups at this position might increase the activity. The red contour at 4-position of phenyl ring indicated that introduction of a negative charge group at this position might increase activity. These conclusions were similar to the predictions in

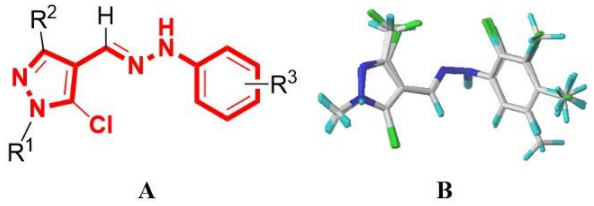

Fig. 4 Common substructure and alignment of training set.

Table 5 PLS statistics of CoMFA and CoMSIA model

PLS statistics	CoMFA	CoMSIA	Validation criteria
q^{2a}	0.575	0.667	>0.5
r^{2b}	0.961	0.962	>0.8
s^c	0.064	0.066	
ONC[d]	5	6	
Steric[e]	0.684	0.136	
Electrostatic[f]	0.316	0.329	
Donor[g]		0.071	
Acceptor[g]		0.056	
Hydrophobic[h]		0.408	

[a] Cross-validated correlation coefficient. [b] Noncross-validated correlation coefficient. [c] Standard error of estimate. [d] Optimum number of principal components. [e] Steric field contribution. [f] Electrostatic field contribution. [g] Donor and acceptor, of hydrogen bond fields contribution, respectively. [h] Hydrophobic field contribution.

the CoMFA model, but there still was some difference between the steric fields. The green contour in Fig. 5C illustrated that adding bulky groups at the phenyl ring might increase the activity.

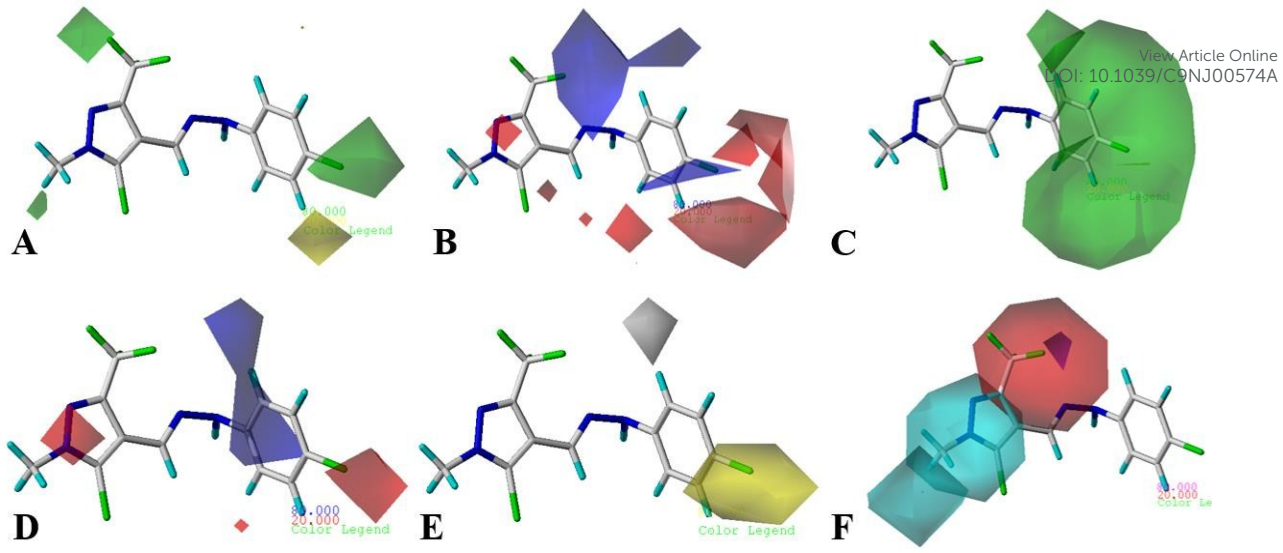

Fig. 5 CoMFA and CoMSIA contour maps. CoMFA model: (A) Green and yellow mean sterically favored and disfavored areas, respectively; (B) Red and blue mean negative charge favored and disfavored areas, respectively. CoMSIA model: Colors in (C) and (D) have the same meanings as maps (A) and (B) in CoMFA model, respectively; (E) Yellow and gray mean hydrophobic favored and disfavored areas, respectively; (F) Cyan and magenta mean H-bond donor and acceptor favored area, respectively, and purple and red mean H-bond donor and acceptor disfavored areas, respectively.

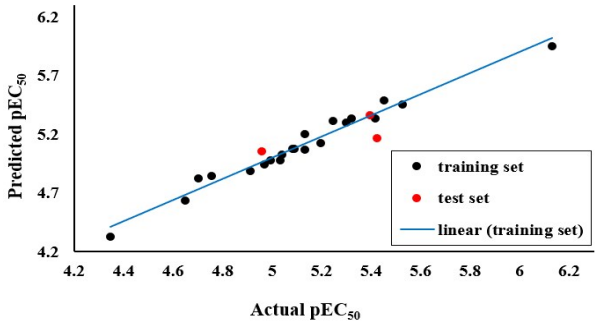

Fig. 6 Correlations between CoMFA predicted and experimental pEC_{50}.

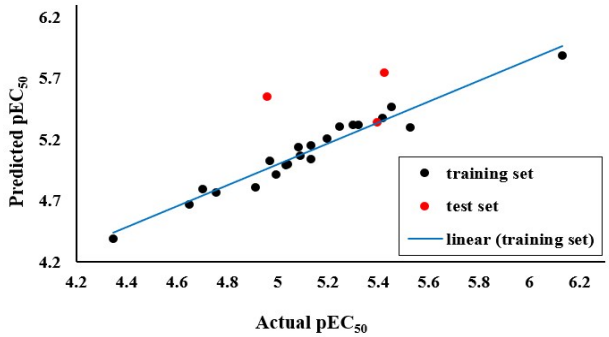

Fig. 7 Correlations between CoMSIA predicted and experimental pEC_{50}.

In the hydrophobic CoMFA map (Fig. 5E), the yellow contour around 4-position of phenyl ring indicated that hydrophobic group was favored at this position. For example, the compounds **7d**, **7f**, **7g**, **7m**, **7o**, **8d**, and **8g** (with 4-halogen at phenyl ring) exhibited higher antifungal activity than the compounds **7a**, **7h**, **7j**, **7p**, and **8a** (with methyl or no substitution at phenyl ring). The grey contour around 2-position of phenyl ring concluded that hydrophobic groups played a disfavored role at these positions on antifungal activity. This explained that the compounds **7b, 7k**, and **8b** had not good fungicidal activity

In the hydrogen bond donor and acceptor CoMSIA contour map (Fig. 5F), the cyan contours around pyrazole ring suggested that hydrogen bond donor was favored at this region. Meanwhile, the magenta contour around 3-position of pyrazole ring indicated that hydrogen bond acceptor was favored. In this model, hydrogen bond was not the key factor (donor and acceptor field contributions were 0.071 and 0.056, respectively). So the introduction of hydrogen atom, methyl and trifluoromethyl group at 1,3-position of pyrazole ring has limited effect on anti-*R. solani* activity.

The analysis of contour maps for CoMFA and CoMSIA models suggested that the antifungal activity of target compounds against *R. solani* was mainly related to steric field, electrostatic field, and hydrophobic field. It can be summarized as following three conclusions. First, the introduction of bulky groups with negative charge at 4-position of phenyl ring could observably improve the fungicidal activity. Second, the bulky groups with hydrophobicity at 2-position of phenyl ring played an unfavorable role on antifungal activity. Finally, the introduction of bulky groups with negative charge at pyrazole ring could improve the fungicidal activity, which confirms the original intention of introducing a chlorine atom at the 5-position of pyrazole ring.

Experimental

General

All melting points of the title compounds were determined on an uncorrected WRS-1B digital melting point apparatus (Jingmi Science, China). ^{1}H NMR and ^{13}C NMR spectra were measured on a AV 400 MHz spectrometer (Bruker, Germany) using DMSO-*d6* as solvent and TMS as internal standard. Mass spectra were recorded on a Triple TOF 5600 plus spectrometer

(AB SCIEX, America). The compound samples prepared with KBr disk were gauged on a Nicolet 380 FT-IR spectrometer (Thermo, America) to obtain the corresponding infrared spectra. The progress of the reactions was monitored by thin layer chromatography (Yuhua, China). All the reagents and solvents purchased from commercial suppliers were analytically or chemically pure and were not further purified.

General procedure for synthesis of 3,5-dichloro-1*H*-pyrazole-4-carbaldehydes 3a and 3b

Diethyl malonate **1** (19.2 g, 0.12 mol) was added to anhydrous ethanol (150 mL) in a 250 mL three-necked flask equipped with a mechanical stirring. And 80% hydrazine hydrate (5.6 g, 0.09 mol) was added dropwise into the mixture at room temperature and the resulting solution was stirring for 5 h. After the end of the reaction, the white solid was filtrated and discarded, and the filtrate was evaporated off under reduced pressure to give colorless liquid. The liquid was stood at 4 ℃ for 1 h. The produced precipitate was filtered and dried to obtain a white solid.

Then, the white solid (4.4 g, 0.03 mol) was dissolved in methanol (100 mL) in a 250 mL three-necked flask equipped with a mechanical stirring, and newly prepared sodium methoxide solution (0.7 g of Na was dissolved in 100 mL of anhydrous methanol) was added dropwise to the resulting solution at room temperature. After completion of the dropwise addition, the reaction mixture was refluxed for 8 h, filtered while the solution was still hot, and distilled off to give a yellow solid. The solid was acidified to pH 2-3 with concentrated hydrochloric acid. And the mixture was allowed to stand at 4 ℃. The precipitate was filtered, washed by ice water, and dried to obtain the compound **2a** in a yield of 38.2%. The compound **2b** was synthesized using a similar method with 40% aqueous solution of methylhydrazine as one of the raw materials.

DMF (14.6 g, 0.2 mol) was cooled down to 0 ℃, then $POCl_3$ (30.6 g, 0.2 mol) was slowly added dropwise while stirring and cooling, the mixture was kept stirring at room temperature for 1 h. The compound **2a** (5 g, 0.05 mol) was added to the reactor in portions. The reaction solution was heated and kept at 50 ℃ for 5 h, then kept at 120 ℃ for another 10 h. The solvent was subsequently poured into 200 mL ice water while stirring, and NaOH solid was slowly added to adjust pH to 6–7. The mixture was extracted with 3×100 mL of ethyl acetate. The organic layer was washed with water, dried and concentrated to obtain a crude product as yellow oil. The crude product was purified by column chromatography with a suitable solvent as the eluent (ethyl acetate: petroleum ether = 1: 4, v/v) to give the compound **3a** as a white solid. The compound **3b** was synthesized using a similar method.

3,5-Dichloro-1*H*-pyrazole-4-carbaldehyde (**3a**): White powder; yield: 40.1%; ^{1}H NMR (400 MHz, DMSO-*d6*) *δ*: 14.77 (s, 1H, NH), 9.77 (s, 1H, CHO).

3,5-Dichloro-1-methyl-1*H*-pyrazole-4-carbaldehyde (**3b**): White powder; yield: 38.4%; ^{1}H NMR (400 MHz, DMSO-*d6*) *δ*: 9.77 (s, 1H, CHO), 3.86 (s, 3H, CH_3).

General procedure for synthesis of 5-chloro-1-methyl-1*H*-pyrazole-4-carbaldehydes 6a and 6b

Methyl 4,4,4-trifluoroacetoacetate (11.6 g, 0.1 mol) was added to anhydrous ethanol (100 mL) in a 250 mL three-necked flask equipped with a mechanical stirring. And 40% aqueous solution of methylhydrazine (11.5 g, 0.1 mol) was added dropwise into the mixture at room temperature. The resulting solution was refluxed for 8 h. Then the reaction mixture was filtered while the solution was still hot, and the solvent was evaporated under reduced pressure to give the product **5a** as a yellow solid. The compound **5b** was synthesized in a similar method with methyl acetoacetate as one of the raw materials.

DMF (14.6 g, 0.2 mol) was cooled down to 0 ℃, then $POCl_3$ (45.9 g, 0.3 mol) was slowly added dropwise under stirring and ice-cooling, and the mixture kept stirring at room temperature for 1 h. Compound **5a** (16.6 g, 0.1 mol) was added to the reactor in portions. The reaction solution was firstly heated to 50 ℃ and reacted for 5 h, then heated to 90 ℃ and reacted for another 5 h. Subsequently, the solvent was poured into 200 mL ice water while stirring. The resulting solution was neutralized to pH 6–7 with NaOH, crystallized from the solution, filtrated and dried to give the compound **6a**. The compound **6b** was synthesized using a similar method.

5-Chloro-3-trifluoromethyl-1-methyl-1*H*-pyrazole-4-carbaldehyde (**6a**): Yellow powder; yield: 78.1%; ^{1}H NMR (400 MHz, DMSO- *d6*) *δ*: 9.83 (s, 1H), 3.95 (s, 3H).

5-Chloro-1,3-dimethyl-1*H*-pyrazole-4-carbaldehyde (**6b**): White powder; yield: 86.4%; ^{1}H NMR (400 MHz, DMSO-*d6*) *δ*: 9.73 (s, 1H), 3.95 (s, 3H), 2.47 (s, 3H).

General procedure for synthesis of target compounds 7 and 8

Phenylhydrazine (0.33 g, 3 mmol) and compound **3a** (0.5 g, 3 mmol) were dissolved in ethanol (15 mL), 1 drop of acetic acid was added dropwise as a catalyst. The mixture was refluxed for 2 h. By distillation under reduced pressure, the solvent was evaporated to give a crude product, which was recrystallized from ethyl acetate and petroleum ether (1: 8, v/v) to give a yellow solid **7a**. In a similar manner, the target compounds **7b**–**7q** and **8a**–**8g** were synthesized.

(*E*)-3,5-Dichloro-4-((2-phenylhydrazono)methyl)-1*H*-pyrazole (**7a**): Yellow powder; yield: 53.36%; m.p. 130.0–131.8 ℃; IR (KBr, cm^{-1}) *v*: 3317, 3120, 2920, 1599, 1519, 1489, 1254, 1131, 988, 744, 667; ^{1}H NMR (400 MHz, DMSO-*d6*) *δ*: 14.01 (s, 1H), 10.36 (s, 1H), 7.69 (s, 1H), 7.21 (t, *J* = 7.8 Hz, 2H), 7.01 (d, *J* = 7.9 Hz, 2H), 6.74 (t, *J* = 7.2 Hz, 1H); ^{13}C NMR (100 MHz, DMSO-*d6*) *δ*: 145.64, 129.58, 128.77, 126.20, 119.18, 112.24, 111.19; HR-MS (ESI): m/z calcd for $C_{10}H_9Cl_2N_4$ ([M+H]$^+$) 255.0199, found 255.0196.

(*E*)-3,5-Dichloro-4-((2-(2-chlorophenyl)hydrazono)methyl)-1*H*-pyrazole(**7b**): Yellow powder; yield: 61.17%; m.p. 225.1–227.8 ℃; IR (KBr, cm^{-1}) *v*: 3310, 3107, 2879, 1597, 1517, 1457, 1291, 1139, 988, 737, 711; ^{1}H NMR (400 MHz, DMSO-*d6*) *δ*: 14.11 (s, 1H), 10.02 (s, 1H), 8.19 (s, 1H), 7.49 (d, *J* = 8.2 Hz, 1H), 7.32 (d, *J* = 7.9 Hz, 1H), 7.25 (t, *J* = 7.7 Hz, 1H), 6.78 (t, *J* = 7.6 Hz, 1H); ^{13}C NMR (100 MHz, DMSO-*d6*) *δ*: 141.83, 130.46,

View Article Online DOI: 10.1039/C9NJ00574A

129.79, 128.52, 119.97, 116.38, 114.20, 111.01; HR-MS (ESI): m/z calcd for $C_{10}H_8Cl_3N_4$ ([M+H]$^+$) 288.9809, found 288.9810.

(*E*)-3,5-Dichloro-4-((2-(3-chlorophenyl)hydrazono)methyl)-1*H*-pyrazole (**7c**): Yellow powder; yield: 65.02%; m.p. 164.5–167.2 ℃; IR (KBr, cm^{-1}) *v*: 3321, 3127, 2921, 1596, 1520, 1388, 1244, 1131, 990, 763, 677; ^{1}H NMR (400 MHz, DMSO-*d6*) *δ*: 12.49 (s, 1H), 10.07 (s, 1H), 7.71 (s, 1H), 7.17 (t, *J* = 8.0 Hz, 1H), 7.03 (s, 1H), 6.85 (d, *J* = 8.2 Hz, 1H), 6.69 (d, *J* = 7.8, 1.2 Hz, 1H); ^{13}C NMR (100 MHz, DMSO-*d6*) *δ*: 147.05, 134.30, 131.21, 127.78, 118.58, 111.53, 110.93, 110.84; HR-MS (ESI): m/z calcd for $C_{10}H_8Cl_3N_4$ ([M+H]$^+$) 288.9809, found 288.9807.

(*E*)-3,5-Dichloro-4-((2-(4-chlorophenyl)hydrazono)methyl)-1*H*-pyrazole (**7d**): Grey-green powder; yield: 64.80%; m.p. 134.1–135.4 ℃; IR (KBr, cm^{-1}) *v*: 3303, 3131, 2911, 1597, 1516, 1479, 1253, 1132, 991, 797, 634; ^{1}H NMR (400 MHz, DMSO-*d6*) *δ*: 14.11 (s, 1H), 10.48 (s, 1H), 7.70 (s, 1H), 7.24 (dd, *J* = 8.7, 2.4 Hz, 2H), 7.04–6.96 (m, 2H); ^{13}C NMR (100 MHz, DMSO-*d6*) *δ*: 144.55, 129.39, 127.13, 122.42, 113.63, 110.97; HR-MS (ESI): m/z calcd for $C_{10}H_8Cl_3N_4$ ([M+H]$^+$) 288.9809, found 288.9807.

(*E*)-3,5-Dichloro-4-((2-(2-fluorophenyl)hydrazono)methyl)-1*H*-pyrazole (**7e**): Brown powder; yield: 60.11%; m.p.202.5–204.1 ℃; IR (KBr, cm^{-1}) *v*: 3315, 3107, 2917, 1625, 1548, 1469, 1387, 1255, 1127, 990, 896, 741; ^{1}H NMR (400 MHz, DMSO-*d6*) *δ*: 14.13 (s, 1H), 10.28 (s, 1H), 8.01 (s, 1H), 7.45 (dd, *J* = 12.0, 4.6 Hz, 1H), 7.17–7.04 (m, 2H), 6.74 (ddd, *J* = 9.0, 7.6, 1.4 Hz, 1H); ^{13}C NMR (100 MHz, DMSO-*d6*) *δ*: 150.53, 148.16, 133.81 (d, *J* = 9.7 Hz), 129.29, 125.45 (d, *J* = 3.0 Hz), 118.95 (d, *J* = 6.6 Hz), 115.44 (d, *J* = 17.5 Hz), 114.03 (d, *J* = 3.3 Hz), 111.02; HR-MS (ESI): m/z calcd for $C_{10}H_8Cl_2FN_4$ ([M+H]$^+$) 273.0105, found 273.0094.

(*E*)-3,5-Dichloro-4-((2-(4-fluorophenyl)hydrazono)methyl)-1*H*-pyrazole (**7f**): Yellow powder; yield: 65.37%; m.p. 102.3–103.9 ℃; IR (KBr, cm^{-1}) *v*: 3307, 3123, 2968, 1508, 1389, 1216, 1133, 992, 817, 772, 658; ^{1}H NMR (400 MHz, DMSO-*d6*) *δ*: 14.09 (s, 1H), 10.36 (s, 1H), 7.67 (s, 1H), 7.06 (t, *J* = 8.8 Hz, 2H), 6.99 (dd, *J* = 9.0, 4.8 Hz, 2H); ^{13}C NMR (100 MHz, DMSO-*d6*) *δ*: 157.47, 155.15, 142.34, 126.27, 116.21, 115.99, 113.15, 113.08, 111.11; HR-MS (ESI): m/z calcd for $C_{10}H_8Cl_2FN_4$ ([M+H]$^+$) 273.0105, found 273.0094.

(*E*)-4-((2-(4-Bromophenyl)hydrazono)methyl)-3,5-dichloro-1*H*-pyrazole (**7g**): Yellow powder; yield: 63.19%; m.p. 168.8–170.4 ℃; IR (KBr, cm^{-1}) *v*: 3307, 3131, 2969, 1507, 1388, 1216, 1132, 991, 816, 772, 657; ^{1}H NMR (400 MHz, DMSO-*d6*) *δ*: 14.13 (s, 1H), 10.52 (s, 1H), 7.70 (s, 1H), 7.36 (d, *J* = 8.6 Hz, 2H), 6.95 (d, *J* = 8.6 Hz, 2H); ^{13}C NMR (100 MHz, DMSO-*d6*) *δ*: 144.92, 132.21, 127.24, 114.15, 110.96, 109.98; HR-MS (ESI): m/z calcd for $C_{10}H_8Cl_2BrN_4$ ([M+H]$^+$) 334.9280, found 334.9279.

(*E*)-3,5-Dichloro-4-((2-(p-tolyl)hydrazono)methyl)-1*H*-pyrazole (**7h**): Red powder; yield: 50.31%; m.p. 110.3–111.7 ℃; IR (KBr, cm^{-1}) *v*: 3310, 2971, 2900, 1674, 1508, 1393, 1250, 1075, 977, 810, 774; ^{1}H NMR (400 MHz, DMSO-*d6*) *δ*: 14.06 (s, 1H), 9.77 (s, 1H), 7.65 (s, 1H), 7.02 (d, *J* = 8.2 Hz, 2H), 6.91 (d, *J* = 8.4 Hz, 2H), 2.20 (s, 3H); ^{13}C NMR (100 MHz, DMSO-*d6*) *δ*: 140.97, 136.30, 131.11, 129.00, 128.55, 126.63, 122.57, 116.84, 115.14, 111.66, 37.13; HR-MS (ESI): m/z calcd for $C_{11}H_{11}Cl_2N_4$ ([M+H]$^+$) 269.0355, found 269.0346.

(*E*)-3,5-Dichloro-4-((2-(3,4-dimethylphenyl)hydrazono)methyl)-1*H*-pyrazole (**7i**): Green powder; yield: 53.16%; m.p. 121.6–122.8 ℃; IR (KBr, cm^{-1}) *v*: 3123, 2970, 2900, 1609, 1498, 1393, 1259, 1075, 1065, 772; ^{1}H NMR (400 MHz, DMSO-*d6*) *δ*: 14.12 (s, 1H), 10.18 (s, 1H), 7.64 (s, 1H), 6.96 (d, *J* = 8.1 Hz, 1H), 6.82-6.69 (m, 2H), 2.16 (s, 3H), 2.12 (s, 3H); ^{13}C NMR (100 MHz, DMSO-*d6*) *δ*: 143.65, 137.03, 135.71, 130.51, 126.61, 125.51, 125.13, 113.69, 112.16, 109.74, 20.32, 19.04; HR-MS (ESI): m/z calcd for $C_{12}H_{13}Cl_2N_4$ ([M+H]$^+$) 283.0512, found 283.0505.

(*E*)-3,5-Dichloro-1-methyl-4-((2-phenylhydrazono)methyl)-1*H*-pyrazole (**7j**): Yellow powder; yield: 59.24%; m.p. 124.6–125.9 ℃; IR (KBr, cm^{-1}) *v*: 3249, 2987, 2901, 2901, 1598, 1539, 1493, 1402, 1256, 886, 774; ^{1}H NMR (400 MHz, DMSO-*d6*) *δ*: 10.38 (s, 1H), 7.67 (s, 1H), 7.21 (t, *J* = 7.8 Hz, 2H), 7.01 (d, *J* = 7.7 Hz, 2H), 6.73 (dd, *J* = 14.4, 7.1 Hz, 1H), 3.81 (s, 3H); ^{13}C NMR (100 MHz, DMSO-*d6*) *δ*: 145.58, 135.82, 129.58, 126.07, 125.78, 119.22, 112.24, 111.99, 37.07; HR-MS (ESI): m/z calcd for $C_{11}H_{11}Cl_2N_4$ ([M+H]$^+$) 269.0355, found 269.0350.

(*E*)-3,5-Dichloro-4-((2-(2-chlorophenyl)hydrazono)methyl)-1-methyl-1*H*-pyrazole (**7k**): Yellow powder; yield: 71.19%; m.p. 123.5–124.7 ℃; IR (KBr, cm^{-1}) *v*: 3237, 2984, 2896, 1591, 1537, 1458, 1295, 1244, 1030, 897, 740; ^{1}H NMR (400 MHz, DMSO-*d6*) *δ*: 10.03 (s, 1H), 8.18 (s, 1H), 7.49 (d, *J* = 8.2 Hz, 1H), 7.32 (d, *J* = 7.9 Hz, 1H), 7.25 (t, *J* = 7.7 Hz, 1H), 6.79 (t, *J* = 7.6 Hz, 1H), 3.82 (s, 3H); ^{13}C NMR (100 MHz, DMSO-*d6*) *δ*: 141.81, 136.26, 130.31, 129.74, 128.47, 126.38, 119.93, 116.42, 114.22, 111.86, 37.05; HR-MS (ESI): m/z calcd for $C_{11}H_{10}Cl_3N_4$ ([M+H]$^+$) 302.9966, found 302.9961.

(*E*)-3,5-Dichloro-4-((2-(3-chlorophenyl)hydrazono)methyl)-1-methyl-1*H*-pyrazole (**7l**): Yellow powder; yield: 67.06%; m.p. 151.9–153.6 ℃; IR (KBr, cm^{-1}) *v*: 3257, 2988, 2896, 1592, 1543, 1392, 1241, 1084, 927, 849, 780, 686; ^{1}H NMR (400 MHz, DMSO-*d6*) *δ*: 10.59 (s, 1H), 7.69 (s, 1H), 7.22 (t, *J* = 8.0 Hz, 1H), 7.01 (s, 1H), 6.92 (d, *J* = 8.2 Hz, 1H), 6.76 (dd, *J* = 7.8, 1.2 Hz, 1H), 3.81 (s, 3H); ^{13}C NMR (100 MHz, DMSO-*d6*) *δ*: 147.02, 136.02, 134.30, 131.19, 127.64, 126.15, 118.61, 111.68, 111.57, 110.94, 37.07; HR-MS (ESI): m/z calcd for $C_{11}H_{10}Cl_3N_4$ ([M+H]$^+$) 302.9966, found 302.9961.

(*E*)-3,5-Dichloro-4-((2-(4-chlorophenyl)hydrazono)methyl)-1-methyl-1*H*-pyrazole (**7m**): Yellow powder; yield: 65.20%; m.p. 159.6–161.8 ℃; IR (KBr, cm^{-1}) *v*: 3232, 2988, 2896, 1595, 1538, 1408, 1130, 1097, 826, 781; ^{1}H NMR (400 MHz, DMSO-*d6*) *δ*: 10.51 (s, 1H), 7.68 (s, 1H), 7.25 (d, *J* = 8.7 Hz, 2H), 7.00 (d, *J* = 8.7 Hz, 2H), 3.82 (d, *J* = 9.9 Hz, 3H); ^{13}C NMR (100 MHz, DMSO-*d6*) *δ*: 144.51, 135.96, 129.37, 126.98, 125.98, 122.47, 113.63, 111.80, 37.05; HR-MS (ESI): m/z calcd for $C_{11}H_{10}Cl_3N_4$ ([M+H]$^+$) 302.9966, found 302.9959.

(*E*)-3,5-Dichloro-4-((2-(2-fluorophenyl)hydrazono)methyl)-1-methyl-1*H*-pyrazole (**7n**): Yellow powder; yield: 61.58%; m.p. 123.3–124.6 ℃; IR (KBr, cm^{-1}) *v*: 3261, 2984, 2896, 1627, 1543, 1391, 1255, 1125, 1081, 906, 749; ^{1}H NMR (400 MHz, DMSO-*d6*) *δ*: 10.31 (s, 1H), 7.98 (s, 1H), 7.44 (t, *J* = 7.7 Hz, 1H), 7.17-7.06 (m, 2H), 6.76 (ddd, *J* = 9.2, 6.3, 1.5 Hz, 1H), 3.81 (s, 3H); ^{13}C NMR (100 MHz, DMSO-*d6*) *δ*: 149.40 (d, *J* = 238.9 Hz), 136.10, 133.80 (d, *J* = 9.7 Hz), 129.21, 126.21, 125.44 (d, *J* = 3.0 Hz), 119.00 (d, *J* = 6.7 Hz), 115.42 (d, *J* = 17.5 Hz), 114.10,

111.87, 37.06; HR-MS (ESI): m/z calcd for $C_{11}H_{10}Cl_2FN_4$ ([M+H]$^+$) 287.0261, found 287.0255.

(*E*)-3,5-Dichloro-4-((2-(4-fluorophenyl)hydrazono)methyl)-1-methyl-1*H*-pyrazole (**7o**): Yellow powder; yield: 67.23%; m.p. 141.3–142.6 ℃; IR (KBr, cm^{-1}) *v*: 3307, 2984, 2901, 1627, 1544, 1499, 1407, 1258, 1066, 818, 772; ^{1}H NMR (400 MHz, DMSO-*d6*) *δ*: 10.40 (s, 1H), 7.65 (s, 1H), 7.06 (t, *J* = 8.9 Hz, 2H), 6.99 (dd, *J* = 9.1, 4.8 Hz, 2H), 3.81 (s, 3H); ^{13}C NMR (100 MHz, DMSO-*d6*) *δ*: 156.32 (d, *J* = 233.9 Hz), 142.28, 135.81, 126.12, 125.78, 116.09 (d, *J* = 22.4 Hz), 113.13 (d, *J* = 7.5 Hz), 111.94, 37.05; HR-MS (ESI): m/z calcd for $C_{11}H_{10}Cl_2FN_4$ ([M+H]$^+$) 287.0261, found 287.0254.

(*E*)-3,5-Dichloro-1-methyl-4-((2-(*p*-tolyl)hydrazono)methyl) -1*H*-pyrazole (**7p**): Yellow powder; yield: 70.31%; m.p. 162.3–164.2 ℃; IR (KBr, cm^{-1}) *v*: 3245, 2992, 2892, 1611, 1536, 1401, 1253, 1066, 813, 775,607; ^{1}H NMR (400 MHz, DMSO-*d6*) *δ*: 10.27 (s, 1H), 7.63 (d, *J* = 0.6 Hz, 1H), 7.02 (d, *J* = 8.2 Hz, 2H), 6.91 (d, *J* = 8.4 Hz, 2H), 3.80 (s, 3H), 2.20 (s, 3H); ^{13}C NMR (100 MHz, DMSO-*d6*) *δ*: 143.37, 135.74, 129.99, 127.74, 125.58, 125.36, 112.27, 112.11, 37.03, 20.72; HR-MS (ESI): m/z calcd for $C_{12}H_{13}Cl_2N_4$ ([M+H]$^+$) 283.0512, found 283.0498.

(*E*)-3,5-Dichloro-4-((2-(3,4-dimethylphenyl)hydrazono)-methyl)-1-methyl-1*H*-pyrazole (**7q**): Yellow powder; yield: 72.53%; m.p. 160.2–161.4 ℃; IR (KBr, cm^{-1}) *v*: 3232, 2917, 2900, 1586, 1478, 1406, 1251, 1049, 889, 772; ^{1}H NMR (400 MHz, DMSO-*d6*) *δ*: 10.19 (s, 1H), 7.61 (d, *J* = 0.7 Hz, 1H), 6.96 (d, *J* = 8.1 Hz, 1H), 6.80–6.73 (m, 2H), 3.80 (s, 3H), 2.16 (s, 3H), 2.11 (s, 3H); ^{13}C NMR (100 MHz, DMSO-*d6*) *δ*: 143.65, 137.03, 135.71, 130.51, 126.61, 125.51, 125.13, 113.69, 112.16, 109.74, 37.00, 20.32, 19.04; HR-MS (ESI): m/z calcd for $C_{13}H_{15}Cl_2N_4$ ([M+Na]$^+$) 319.0488, found 319.0473.

(*E*)-5-Chloro-1-methyl-4-((2-phenylhydrazono)methyl)-3-(trifluoromethyl)-1*H*-pyrazole (**8a**): Yellow powder; yield: 60.38%; m.p. 113.2–115.1 ℃; IR (KBr, cm^{-1}) *v*: 3319, 2979, 2892, 1598, 1545, 1478, 1291, 1126, 1125, 1077, 889, 693; ^{1}H NMR (400 MHz, DMSO-*d6*) *δ*: 10.51 (s, 1H), 7.76 (s, 1H), 7.22 (t, *J* = 7.8 Hz, 2H), 7.02 (d, *J* = 8.2 Hz, 2H), 6.76 (t, *J* = 7.2 Hz, 1H), 3.91 (s, 3H); ^{13}C NMR (100 MHz, DMSO-*d6*) *δ*: 145.41, 136.38 (q, *J* = 37.6 Hz), 129.61, 127.10, 124.90, 121.59 (d, *J* = 269.0 Hz), 119.51, 113.92, 112.29, 37.54; HR-MS (ESI): m/z calcd for $C_{12}H_{11}ClF_3N_4$ ([M+H]$^+$) 303.0619, found 303.0608.

(*E*)-5-Chloro-4-((2-(2-chlorophenyl)hydrazono)methyl)-1-methyl-3-(trifluoromethyl)-1*H*-pyrazole (**8b**): Yellow powder; yield: 66.84%; m.p. 120.3–121.5 ℃; IR (KBr, cm^{-1}) *v*: 3324, 2988, 2896, 1592, 1507, 1403, 1258, 1164, 1078, 1049, 897, 740; ^{1}H NMR (400 MHz, DMSO-*d6*) *δ*: 10.16 (s, 1H), 8.28 (s, 1H), 7.48 (dd, *J* = 8.2, 1.3 Hz, 1H), 7.34 (dd, *J* = 7.9, 1.2 Hz, 1H), 7.26 (dd, *J* = 11.4, 4.1 Hz, 1H), 6.80 (td, *J* = 7.8, 1.5 Hz, 1H), 3.93 (s, 3H); ^{13}C NMR (100 MHz, DMSO-*d6*) *δ*: 141.67, 136.77 (q, *J* = 37.8 Hz), 129.78, 129.24, 128.46, 127.70, 124.19 (d, *J* = 269.2 Hz), 120.20, 116.56, 114.16, 113.66, 37.52; HR-MS (ESI): m/z calcd for $C_{12}H_{10}Cl_2F_3N_4$ ([M+H]$^+$) 337.0229, found 337.0220.

(*E*)-5-Chloro-4-((2-(3-chlorophenyl)hydrazono)methyl)-1-methyl-3-(trifluoromethyl)-1*H*-pyrazole (**8c**): Yellow powder; yield: 60.38%; m.p. 135.0–136.5 ℃; IR (KBr, cm^{-1}) *v*: 3361, 2979, 2896, 1593, 1540, 1481, 1288, 1077, 911, 769, 721; ^{1}H NMR (400 MHz, DMSO-*d6*) *δ*: 10.72 (s, 1H), 7.77 (s, 1H), 7.23 (t, *J* = 8.0 Hz, 1H), 7.04 (s, 1H), 6.91 (d, *J* = 8.2 Hz, 1H), 6.78 (d, *J* = 7.8 Hz, 1H), 3.92 (s, 3H); ^{13}C NMR (100 MHz, DMSO-*d6*) *δ*: 146.86, 136.30 (q, *J* = 37.8 Hz), 134.33, 131.24, 127.58, 126.45, 121.52 (d, *J* = 268.9 Hz), 118.92, 113.57, 111.65, 110.99, 37.59; HR-MS (ESI): m/z calcd for $C_{12}H_{10}Cl_2F_3N_4$ ([M+H]+) 337.0229, found 337.0217.

(*E*)-5-Chloro-4-((2-(4-chlorophenyl)hydrazono)methyl)-1-methyl-3-(trifluoromethyl)-1*H*-pyrazole (**8d**): Yellow powder; yield: 68.24%; m.p. 145.5–146.3 ℃; IR (KBr, cm^{-1}) *v*: 3357, 2979, 2896, 1593, 1540, 1481, 1403, 1239, 1115, 1077, 988, 769; ^{1}H NMR (400 MHz, DMSO-*d6*) *δ*: 10.64 (s, 1H), 7.76 (s, 1H), 7.26 (d, *J* = 8.5 Hz, 2H), 7.00 (d, *J* = 8.6 Hz, 2H), 3.92 (s, 3H); ^{13}C NMR (100 MHz, DMSO-*d6*) *δ*: 144.33, 136.46 (q, *J* = 37.7 Hz), 129.42, 127.33, 125.82, 122.81, 121.49 (d, *J* = 293.0 Hz), 120.20, 113.68, 37.55; HR-MS (ESI): m/z calcd for $C_{12}H_{10}Cl_2F_3N_4$ ([M+H]$^+$) 337.0229, found 337.0214.

(*E*)-5-Chloro-4-((2-(2-chlorophenyl)hydrazono)methyl)-1,3-dimethyl-1*H*-pyrazole (**8e**): Yellow powder; yield: 65.21%; m.p. 131.7–133.4 ℃; IR (KBr, cm^{-1}) *v*: 3315, 2971, 2901, 1596, 1534, 1453, 1131, 1047, 1027, 777, 735; ^{1}H NMR (400 MHz, DMSO-*d6*) *δ*: 9.78 (s, 1H), 8.23 (s, 1H), 7.41 (d, *J* = 8.2 Hz, 1H), 7.31 (d, *J* = 7.9 Hz, 1H), 7.24 (t, *J* = 7.7 Hz, 1H), 6.75 (t, *J* = 7.6 Hz, 1H), 3.75 (s, 3H), 2.39 (s, 3H); ^{13}C NMR (100 MHz, DMSO-*d6*) *δ*: 145.96, 142.03, 133.55, 129.75, 128.51, 125.96, 119.50, 116.24, 113.88, 112.50, 36.24, 14.85; HR-MS (ESI): m/z calcd for $C_{12}H_{13}Cl_2N_4$ ([M+H]$^+$) 283.0512, found 283.0497.

(*E*)-5-Chloro-4-((2-(3-chlorophenyl)hydrazono)methyl)-1,3-dimethyl-1*H*-pyrazole (**8f**): Yellow powder; yield: 70.04%; m.p. 167.2–168.2 ℃; IR (KBr, cm^{-1}) *v*: 3245, 2984, 2901, 1596, 1540, 1469, 1407, 1066, 922, 758, 679; ^{1}H NMR (400 MHz, DMSO-*d6*) *δ*: 10.38 (s, 1H), 7.76 (s, 1H), 7.21 (t, *J* = 8.0 Hz, 1H), 6.95 (s, 1H), 6.87 (d, *J* = 8.2 Hz, 1H), 6.73 (d, *J* = 7.8 Hz, 1H), 3.75 (s, 3H), 2.37 (s, 3H); ^{13}C NMR (100 MHz, DMSO-*d6*) *δ*: 147.34, 145.81, 134.27, 131.23, 130.88, 125.68, 118.12, 112.33, 111.27, 110.74, 36.26, 14.78; HR-MS (ESI): m/z calcd for $C_{12}H_{13}Cl_2N_4$ ([M+H]$^+$) 283.0512, found 283.0500.

(*E*)-5-Chloro-4-((2-(4-chlorophenyl)hydrazono)methyl)-1,3-dimethyl-1*H*-pyrazole (**8g**): Yellow powder; yield: 67.85%; m.p. 182.5–183.9 ℃; IR (KBr, cm^{-1}) *v*: 3228, 2988, 2892, 1602, 1539, 1483, 1407, 1288, 1079, 814, 776; ^{1}H NMR (400 MHz, DMSO-*d6*) *δ*: 10.30 (s, 1H), 7.75 (s, 1H), 7.23 (d, *J* = 8.6 Hz, 2H), 6.95 (d, *J* = 8.6 Hz, 2H), 3.74 (s, 3H), 2.36 (s, 3H); ^{13}C NMR (100 MHz, DMSO-*d6*) *δ*: 145.74, 144.84, 130.25, 129.36, 125.46, 121.90, 113.40, 112.45, 36.20, 14.82; HR-MS (ESI): m/z calcd for $C_{12}H_{13}Cl_2N_4$ ([M+H]$^+$) 283.0512, found 283.0506.

X-Ray crystal diffraction

The X-ray crystal diffraction was performed with a Bruker Smart APEX II CCD diffractometer. The suitable crystal of compound **8a** was grown from ethanol and water. The crystal data of compound **8a** was measured at 296(2) K. Monochromatic Mo–K*α* radiation (*λ* = 0.71073 Å) was used for the measurements. Absorption corrections using multi *ψ*–scans were applied. The structure was solved using SHELXS-

97.[39] The X-ray data have been deposited at the Cambridge Crystallographic Data Centre with the CCDC number 1846970.

Antifungal activity assay

The target compounds were tested for antifungal acitivity against *F. graminearum, B. cinerea* and *R. solani in vitro* by mycelium growth rate method.[35,40] The tested fungus strains were provided by the Laboratory of Plant Disease Control at Nanjing Agricultural University. Every sample was dissolved in DMSO and mixed with PSA (potato sucrose agar) medium. An equal dose of DMSO in medium was used as the blank control. Meanwhile, the commercial agricultural fungicides carbendazim and penthiopyrad were tested as the positive control at the same concentration. Each 15 mL medium was poured into a 9 cm petri plate with 3 replicates. The fungi were inoculated to the center of the medium and cultured at 25 ℃ for 3–5 days in a dark environment. After a certain incubation period, the diameters of the mycelium colonies were measured, and the inhibitory percentages were calculated. The median effective concentration (EC_{50}) values were calculated using linear-regression analysis.

3D-QSAR study method

The 3D-QSAR model of target compounds was established via built-in QSAR software of Sybyl X-2.1 (Tripos). The energy minimization of target molecular conformations was performed using the Tripos force field and the Gasteiger-Hückel method with the 1000 times iteration and 0.005 kcal mol^{-1} $Å^{-1}$) convergence gradient. The fields properties of both CoMFA and CoMSIA model were calculated using partial least squares analysis (PLS).[35,41]

Conclusions

The substituted phenylhydrazone moieties were introduced to 4-position of 5-chloro-pyrazoles to design and synthesize a series of novel pyrazole derivatives as potent antifungal agents. The target compounds were well characterized by the spectroscopy and single crystal X-ray diffraction. The bioassay results indicated that most of target compounds exhibited obvious fungicidal activity against the tested plant pathogenic fungi. The compounds **7c** and **8d** showed most potent inhibitory activity with the EC_{50} values of 0.68 μg/mL and 0.25 μg mL^{-1} against *B. cinerea* and *R. solani*, respectively, which are superior than the corresponding control drugs carbendazim and penthiopyrad. The CoMFA and CoMSIA models were established for 3D-QSAR study, which showed good predictive ability with satisfactory q^2 and r^2 values. The obtained analytic results from the molecular models provided useful information for further structural modification and optimization of 5-chloro-pyrazole derivatives with a phenylhydrazone moiety to screen new fungal inhibitors with high efficacy.

Conflicts of interest

There are no conflicts of interest to declare.

View Article Online
DOI: 10.1039/C9NJ00574A

Acknowledgements

The authors gratefully acknowledge the financial support of the National Natural Science Foundation of China (No. 31772209) and the Fundamental Research Funds for the Central Universities of China (No. KYTZ201604).

Notes and references

1. Z. Li, S. Chen, S. Zhu, J. Luo, Y. Zhang, Q. Weng, *Molecules,* 2015, **20**, 13941–13957.
2. R. A. Wilso, N. J. Talbot, *Microbiology,* 2009, **155**, 3810–3815.
3. G. Bai, G. Shaner, *Annu. Rev. Phytopathol*., 2004, **42**, 135–161.
4. N. A. Foroud, F. Eudes, *Int. J. Mol. Sci*., 2009, **10**, 147–173.
5. J. N. Sangshetti , D. B. Shinde, *Bioorg. Med. Chem. Lett*., 2010, **20**, 742–745.
6. F. Borges, F. Roleira, N. Milhazes, L. Santana, E. Uriarte, *Curr. Med. Chem*., 2005, **12**, 887–916.
7. K. D. Wehrstedt, P. A. Wandrey, D. Heitkamp, *J. Hazard. Mater*., 2005, **A126**, 1–7.
8. P. Dai, K. Luo, X. Yu, W. -C. Yang, L. Wu, W. -H. Zhang, *Adv. Synth. Catal*., 2018, **360**, 468–473.
9. Y. Wang, Y. -P. Hou, C. -J. Chen, M. -G. Zhou, *Australas. Plant Path*., 2014, **43**, 307–312.
10. G. Bai, G. Shaner, *Plant Disease*, 1994, **78**, 760–766.
11. M. F. El Shehry, M. M. Ghorab, S. Y. Abbas, E. A. Fayed, S. A. Shedid, Y. A. Ammar, *Eur. J. Med. Chem*., 2018, **143**, 1463–1473.
12. S. Mert, R. Kasımoğulları, T. İça, F. Çolak, A. Altun, S.Ok, *Eur. J. Med. Chem*., 2014, **78**, 86–96.
13. C. B. Vicentini, C. Romagnoli, E. Andreotti, D. Mares, *J. Agric. Food. Chem*., 2007, **55**, 10331–10338.
14. H. Dai, G. Li, J. Chen, Y. Shi, S. Ge, C. Fan, H. He, *Bioorg. Med. Chem. Lett*., 2016, **26**, 3818–3821.
15. H. Yu, Y. Cheng, M. Xu, Y. Song, Y. Luo, B. Li, *J. Agric. Food. Chem*., 2016, **64**, 9586–9591.
16. M. Bhat, G. K. Nagaraja, R. Kayarmar, S. K. Peethamber, R. Mohammed Shafeeulla, *RSC Advances*, 2016, **6**, 59375–59388.
17. Y. Fu, M. -X. Wang, D. Zhang, Y. -W. Hou, *RSC Advances*, 2017, **7**, 46858–46865.
18. H. Nagahori, H. Yoshino, Y. Tomigahara, N. Isobe, H. Kaneko, I. Nakatsuka, *J. Agric. Food Chem.,* 2000, **48**, 5754–5759.
19. Y. Yoshikawa, H. Katsuta, J. Kishi, Y. Yanase, *J. Pestic. Sci.,* 2011, **36**, 347–356.
20. L. E. Gomez, L. Srigiriraju, A. Roy, WO 2017086970, 2017-05-26.
21. Z. Zhuang, N. Xu, Z. Zhuang, Y. Liu, Y. Han, J. Fan, *Agrochemicals*, 2016, **55**, 316–319.
22. L. -M. Hu, X. -S. Li, Z. -Y. Chen, Z. -J. Liu, *Chinese J. Org. Chem*., 2003, **23**, 1131–1134.
23. L. -M. Yang, S. -B. Hua, Z. -J. Liu, *Chinese J. Appl. Chem*., 2005, **22**, 829–834.
24. C. -X. Tan, D. -L. Shen, J. -Q. Weng, N. -B. Sun, X. -M. Ou, *Chinese J. Pestic. Sci.*, 2006, **8**, 363–366.
25. J. Wu J, Q. Shi, Z. Chen, M. He, L. Jin, D. Hu, *Molecules*, 2012, **17**, 5139–5150.
26. K. Matsuura, Y. Ishida, T. Kuragano, K. Konishi, *J. Pestic. Sci.,* 1994, **19**, S197–S207.
27. I. F. Eckhard, K. Lehtonen, T. Staub, L. A. Summers, *Aust. J. Chem.*, 1973, **26**, 2705–2710.

28. J. -J. Wang, W. -J. Si, M. Chen, A. -M. Lu, W. -H. Zhang, C. -L. Yang, *J. Pestic. Sci.,* 2017, **42**, 84–92.
29. N. Aggarwal, R. Kumar, C. Srivastva, P. Dureja, J. M. Khurana, *J. Agric. Food Chem*., 2010, **58**, 3056–3061.
30. Y. Liu, H. Song, Y. Huang, J. Li, S. Zhao, Y. Song, P. Yang, Z. Xiao, Y. Liu, Y. Li, S. Hui, H. Shang, *J. Agric. Food Chem*., 2014, **62**, 9987–9999.
31. Z. -C. Dai, Y. -F. Chen, M. Zhang, S. -K. Li, T. -T. Yang, L. Shen, J. -X. Wang, S. -S. Qian, H. -L. Zhu, Y. -H. Ye, *Org. Biomol. Chem*., 2015, **13**, 477–486.
32. X. Wang, Y. -F. Chen, W. Yan, L. -L. Cao, Y. -H. Ye, *Molecules,* 2016, **21**, 1574.
33. M. Zhang, Z. -C. Dai, S. -S. Qian, J. -Y. Liu, Y. Xiao, A. -M. Lu, H. -L. Zhu, J. -X. Wang, Y. -H. Ye, *J. Agric. Food Chem*., 2014, **62**, 9637–9643.
34. Y. Hu, J. Wang, A. Lu, C. Yang, *Bioorg. Med. Chem. Lett*., 2014, **24**, 3772–3776.
35. X. Wang, M. Wang, J Yan, M Chen, A. Wang, Y. Mei, W. Si, C. Yang, *ChemistrySelect*, 2018, **3**, 10663–1069.
36. H. Jung, W. Aman, J. -M. Hah, *Bioorg. Med. Chem. Lett*., 2017, **27**, 2139–2143.
37. J. Wu, Q. Shi, Z. Chen, M. He, L. Jin, D. Hu, *Molecules,* 2012, **17**, 5139–5150.
38. S. Hesse, G. Kirsch, *Tetrahedron Lett*., 2002, **43**, 1213–1215.
39. G. M. Sheldrick, *Acta Crystallogr., Sect. A: Found. Crystallogr.*, 2008, **64**, 112–122.
40. L. -X. Li, J. Jiao, X. -B. Wang, M. Chen, X. -C. Fu, W. -J. Si, C. -L. Yang, *Molecules*, 2018, ***23***, 746.
41. X. Y. Huang, Z. J. Shan, H. L. Zhai, L. N. Li, X. Y. Zhang, *J. Chem. Inf. Model.*, 2011, **51**, 1999–2006.

Novel 5-chloro-pyrazole derivatives containing a phenylhydrazone moiety as potent antifungal agents: Synthesis, crystal structure, biological evaluation and 3D-QSAR study

View Article Online
DOI: 10.1039/C9NJ00574A

Jian Jiao, An Wang, Min Chen, Meng-Qi Wang and Chun-Long Yang

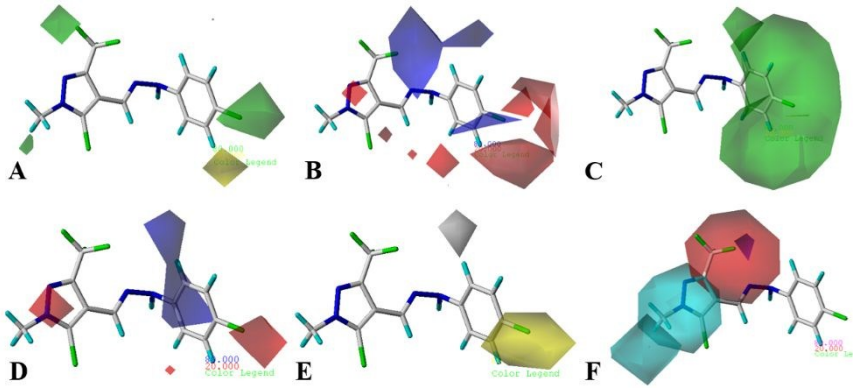

Novel 5-chloro-pyrazole derivatives containing a phenylhydrazone moiety were designed and synthesized. Some target compounds showed potent fungicidal activity. The 3D-QSAR models provided useful information for structural optimization.